

1-1-2014

Peroxisome proliferator-activated receptor δ agonist GW1516 attenuates diet-induced aortic inflammation, insulin resistance, and atherosclerosis in low-density lipoprotein receptor knockout mice

Lazar A. Bojic
Robarts Research Institute

Amy C. Burke
Robarts Research Institute

Sanjiv S. Chhoker
Robarts Research Institute

Dawn E. Telford
Robarts Research Institute

Brian G. Sutherland
Robarts Research Institute

See next page for additional authors

Follow this and additional works at: <https://ir.lib.uwo.ca/paedpub>

Citation of this paper:

Bojic, Lazar A.; Burke, Amy C.; Chhoker, Sanjiv S.; Telford, Dawn E.; Sutherland, Brian G.; Edwards, Jane Y.; Sawyez, Cynthia G.; Tirona, Rommel G.; Yin, Hao; Pickering, J. Geoffrey; and Huff, Murray W., "Peroxisome proliferator-activated receptor δ agonist GW1516 attenuates diet-induced aortic inflammation, insulin resistance, and atherosclerosis in low-density lipoprotein receptor knockout mice" (2014). *Paediatrics Publications*. 2315.

<https://ir.lib.uwo.ca/paedpub/2315>

Authors

Lazar A. Bojic, Amy C. Burke, Sanjiv S. Chhoker, Dawn E. Telford, Brian G. Sutherland, Jane Y. Edwards, Cynthia G. Sawyez, Rommel G. Tirona, Hao Yin, J. Geoffrey Pickering, and Murray W. Huff

Peroxisome Proliferator–Activated Receptor δ Agonist GW1516 Attenuates Diet-Induced Aortic Inflammation, Insulin Resistance, and Atherosclerosis in Low-Density Lipoprotein Receptor Knockout Mice

Lazar A. Bojic, Amy C. Burke, Sanjiv S. Chhoker, Dawn E. Telford, Brian G. Sutherland, Jane Y. Edwards, Cynthia G. Sawyez, Rommel G. Tirona, Hao Yin, J. Geoffrey Pickering, Murray W. Huff

Objective—The peroxisome proliferator–activated receptor (PPAR) δ regulates systemic lipid homeostasis and inflammation. However, the ability of PPAR δ agonists to improve the pathology of pre-established lesions and whether PPAR δ activation is atheroprotective in the setting of insulin resistance have not been reported. Here, we examine whether intervention with a selective PPAR δ agonist corrects metabolic dysregulation and attenuates aortic inflammation and atherosclerosis.

Approach and Results—Low-density lipoprotein receptor knockout mice were fed a chow or a high-fat, high-cholesterol (HFHC) diet (42% fat, 0.2% cholesterol) for 4 weeks. For a further 8 weeks, the HFHC group was fed either HFHC or HFHC plus GW1516 (3 mg/kg per day). GW1516 significantly attenuated pre-established fasting hyperlipidemia, hyperglycemia, and hyperinsulinemia, as well as glucose and insulin intolerance. GW1516 intervention markedly reduced aortic sinus lesions and lesion macrophages, whereas smooth muscle α -actin was unchanged and collagen deposition enhanced. In aortae, GW1516 increased the expression of the PPAR δ -specific gene *Afp* but not PPAR α - or γ -specific genes. GW1516 intervention decreased the expression of aortic proinflammatory M1 cytokines, increased the expression of the anti-inflammatory M2 cytokine *Arg1*, and attenuated the *iNos/Arg1* ratio. Enhanced mitogen-activated protein kinase signaling, known to induce inflammatory cytokine expression in vitro, was enhanced in aortae of HFHC-fed mice. Furthermore, the HFHC diet impaired aortic insulin signaling through Akt and forkhead box O1, which was associated with elevated endoplasmic reticulum stress markers CCAAT-enhancer-binding protein homologous protein and 78kDa glucose regulated protein. GW1516 intervention normalized mitogen-activated protein kinase activation, insulin signaling, and endoplasmic reticulum stress.

Conclusions—Intervention with a PPAR δ agonist inhibits aortic inflammation and attenuates the progression of pre-established atherosclerosis. (*Arterioscler Thromb Vasc Biol.* 2014;34:52-60.)

Key Words: atherosclerosis ■ inflammation ■ insulin resistance ■ lipids

The principal cause of mortality in patients with type 2 diabetes mellitus is atherosclerosis,¹ a chronic inflammatory disease that is the primary precursor underlying most cardiovascular events.² Although the molecular and pathophysiological links between type 2 diabetes mellitus and atherosclerosis are not fully understood, a crucial factor is likely insulin resistance.³ This is, in part, because of the promotion of multiple independent risk factors associated with cardiovascular disease, including obesity, hypertension, and dyslipidemia.³ Dyslipidemia associated with insulin resistance is characterized by increased plasma triglyceride (TG)-rich very-low-density lipoprotein (VLDL) and cholesteryl ester-rich low-density lipoprotein (LDL), both of which can permeate a compromised endothelium and initiate atherogenesis.^{3,4}

Therapeutic strategies to reduce plasma LDL have proven effective in reducing cardiovascular events.⁵ However, a significant unmet medical need persists, making VLDL-lowering strategies an attractive therapeutic target.

See accompanying editorial on page 5

Subendothelial retention of atherogenic lipoproteins leads to a series of maladaptive immune responses culminating in the development of macrophage foam cells.^{2,4} Foam cells play a critical role in the progression of fatty streaks toward more advanced lesions. In particular, M1 macrophages secrete inflammatory effector cytokines such as interleukin (IL)-1 β and tumor necrosis factor- α , driven predominantly by mitogen-activated protein kinase (MAPK) and nuclear factor

Received on: May 11, 2013; final version accepted on: October 8, 2013.

From the Department of Vascular Biology, Robarts Research Institute (L.A.B., A.C.B., S.S.C., D.E.T., B.G.S., J.Y.E., C.G.S., H.Y., J.G.P., M.W.H.), London, Ontario, Canada; and Departments of Biochemistry (L.A.B., A.C.B., S.S.C., J.G.P., M.W.H.), Medicine (D.E.T., J.Y.E., C.G.S., R.G.T., J.G.P., M.W.H.), and Physiology and Pharmacology (R.G.T.), The University of Western Ontario, London, Ontario, Canada.

The online-only Data Supplement is available with this article at <http://atvb.ahajournals.org/lookup/suppl/doi:10.1161/ATVBAHA.113.301830/-DC1>.

Correspondence to Murray W. Huff, PhD, Robarts Research Institute, Room 4222, The University of Western Ontario, 1151 Richmond St. N., London, Ontario, Canada N6A 5B7. E-mail mhuff@uwo.ca

© 2013 American Heart Association, Inc.

Arterioscler Thromb Vasc Biol is available at <http://atvb.ahajournals.org>

DOI: 10.1161/ATVBAHA.113.301830

Nonstandard Abbreviations and Acronyms

ER	endoplasmic reticulum
FoxO1	forkhead box O1
HFHC	high fat, high cholesterol
LDL	low-density lipoprotein
<i>Ldlr</i>^{-/-}	LDL receptor knockout mice
NF-κB	nuclear factor- κ B
PPARδ	peroxisome proliferator-activated receptor δ
SM	smooth muscle
TG	triglyceride
VLDL	very-low-density lipoprotein

(NF)- κ B signaling.⁶ However, insulin signaling, namely the Akt/forkhead box O1 (FoxO1) pathway, may also contribute to arterial inflammation.⁴ In vitro, *Il1 β* is a FoxO1 target gene in macrophages, with fatty acid-induced insulin resistance.⁷ Despite 1 study reporting the contrary,⁸ a growing body of evidence suggests that in vivo, arterial insulin resistance directly promotes atherosclerosis.⁴ Global deletion of Akt1 in apolipoprotein E-deficient mice accelerated coronary artery disease and aortic atherosclerosis, concomitant with significant aortic inflammation.⁹ Hematopoietic deletion of the insulin receptor in LDL receptor knockout (*Ldlr*^{-/-}) mice amplified atherogenesis, an effect attributed to impaired macrophage Akt signaling.¹⁰ Furthermore, increased areas of apoptotic macrophages and necrotic core have been visualized in atherosclerotic lesions from patients with type 2 diabetes mellitus.¹¹ Collectively, these studies support the concept that arterial insulin resistance promotes inflammation and atherogenesis.

Peroxisome proliferator-activated receptors (PPARs) are a class of ligand-dependant transcription factors involved in the regulation of metabolic and inflammatory signaling.¹² Three isoforms exist (α , γ , δ), which exhibit overlapping but distinct patterns of tissue distribution and function.¹² Although PPAR δ has been considered the most enigmatic PPAR, this receptor has emerged as an important regulator of cellular lipid homeostasis and inflammatory responses.¹³ In cultured macrophages, PPAR δ activation inhibits both macrophage lipid accumulation and pro-inflammatory cytokine expression in response to human VLDL.¹⁴ Furthermore, TG accumulation was decreased via angiotensin-like 4-mediated inhibition of macrophage lipoprotein lipase and enhanced carnitine palmitoyltransferase 1 α -stimulated fatty acid β -oxidation. Attenuated cytokine expression was mediated through both inhibition of extracellular signal-regulated kinase 1/2 and activation of Akt/FoxO1 signaling.¹⁴ In vivo, Lee et al¹⁵ demonstrated that macrophage deletion of *Ppar δ* in *Ldlr*^{-/-} mice paradoxically decreased atherogenesis. This effect was attributed to the suppression of atherogenic inflammation by liberation of the inflammatory repressor protein B-cell lymphoma-6 because this protein is normally sequestered by the PPAR δ /retinoid X receptor corepressor complex.¹⁵ These studies highlight that deletion of *Ppar δ* mimics the liganded state of the receptor, suggesting that ligand activation may be atheroprotective. However, studies examining the effects of synthetic PPAR δ agonists using prevention protocols in mice have produced a spectrum of results.¹⁶⁻¹⁸ In 1 study, administration of the PPAR δ agonist GW0742 to *Ldlr*^{-/-} mice fed a high-fat diet had no effect on lesion size.¹⁶ In

a second study, GW0742 reduced lesion development in female *Ldlr*^{-/-} mice,¹⁷ although the doses used yielded serum drug levels 2-fold higher than the EC₅₀ values for murine PPAR α and PPAR γ ,¹⁸ raising the possibility that atheroprotection by GW0742 was not PPAR δ specific. In *Ldlr*^{-/-} mice fed a high-fat diet, low doses of GW0742 prevented the development of angiotensin II-accelerated atherosclerosis.¹⁹ The next-generation PPAR δ agonist (GW1516) at PPAR δ -specific doses prevented the development of atherosclerosis in apolipoprotein E-deficient mice fed a high-fat diet, concomitant with reduced aortic inflammatory cytokine expression.¹⁸ Although on balance these studies indicate that PPAR δ -specific agonists prevent the development of atherosclerosis and arterial inflammation, it is unknown whether PPAR δ agonists are atheroprotective in an intervention model with pre-established insulin resistance and atherosclerosis. Furthermore, the effect of PPAR δ activation on lesion pathology, as well as aortic inflammatory signaling cascades, insulin resistance, and endoplasmic reticulum (ER) stress, has not been examined.

In the present study, we use C57BL/6J *Ldlr*^{-/-} mice fed a high-fat, high-cholesterol (HFHC) diet, a model of diet-induced dyslipidemia and insulin resistance. After a diet induction phase, intervention with the addition of the PPAR δ -specific agonist GW1516 to the HFHC diet resulted in reversal of metabolic dysregulation, including reduced plasma lipids, glucose, and insulin and improved glucose and insulin tolerance. Intervention with GW1516 inhibited aortic MAPK and NF- κ B signaling, attenuated aortic inflammation, improved indices of aortic insulin signaling, reduced aortic ER stress, and collectively attenuated the progression of pre-established atherosclerosis.

Materials and Methods

Materials and Methods are available in the online-only Supplement.

Results

GW1516 Improves HFHC-Induced Metabolic Dysregulation in *Ldlr*^{-/-} Mice

Male C57BL/6 *Ldlr*^{-/-} mice were administered an HFHC diet for 4 weeks. The metabolic effects of intervention with the PPAR δ agonist GW1516 were evaluated after an additional 8 weeks (Figure 1A). GW1516 at 3 mg/kg per day resulted in GW nonfasting serum concentrations at the end of the dark and light cycles of 604 \pm 72 and 369 \pm 26 nmol/L, respectively, for a mean concentration of 487 \pm 50 nmol/L. This plasma concentration is below the EC50 for murine PPAR γ (1 μ mol/L) and well below the EC50 for murine PPAR α (2.5 μ mol/L).²⁰ GW1516 intervention significantly attenuated HFHC-induced weight gain without affecting caloric intake (Figure 1A and 1B in the online-only Data Supplement). GW1516 decreased fasting plasma cholesterol, TG, and nonesterified fatty acids compared with 4-week baseline levels, whereas dyslipidemia in mice remaining on the HFHC diet alone continued to progress (Figure 1B). Fast protein liquid chromatography analyses demonstrated that reduced plasma cholesterol in GW1516-treated mice was because of a significant reduction in VLDL cholesterol and a modest but not statistically significant reduction in LDL cholesterol (Figure 1C). GW1516 increased high-density lipoprotein cholesterol by 35% (Figure 1C). The GW1516-mediated

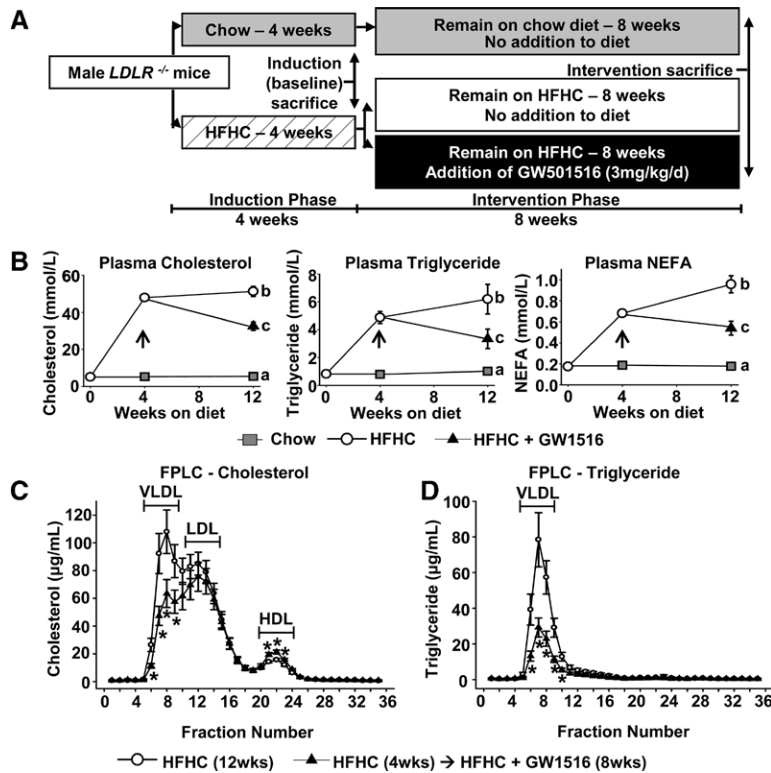


Figure 1. GW1516 intervention improves diet-induced dyslipidemia. Low-density lipoprotein receptor knockout (*Ldlr*^{-/-}) mice were fed standard chow or a high-fat, high-cholesterol (HFHC) diet for 4 weeks. For a subsequent 8 weeks, chow-fed mice remained on chow; the HFHC-fed mice either remained on HFHC alone or HFHC supplemented with GW1516 (GW1516); 3 mg/kg per day. **A**, Experimental timeline for all studies performed. **B**, Plasma cholesterol, triglyceride, and nonesterified fatty acid (NEFA) concentrations were measured at weeks 0, 4, and 12 (8–12/group). Arrows indicate the time of GW1516 intervention. **C** and **D**, Plasma was subjected to fast protein liquid chromatography (FPLC) analysis at week 12, and cholesterol and triglyceride were measured in the eluted fractions (n=3–5/group). Data are presented as mean±SEM. In **B**, different letters indicate significant differences (P<0.05). In **C** and **D**, *indicates significant difference vs HFHC (12 weeks; P<0.05). HDL indicates high-density lipoprotein; LDL, low-density lipoprotein; and VLDL, very-low-density lipoprotein.

reduction in plasma TG was because of a substantial 63% reduction in VLDL-TG (Figure 1D). GW1516 intervention decreased epididymal fat by 11% compared with 4-week baseline and by 35% compared with mice remaining on the HFHC diet alone (Figure IC in the online-only Data Supplement), demonstrating attenuation of adipose tissue accumulation.

GW1516 prevented the increase in fasting blood glucose (from week 4 to week 12) and completely normalized impaired glucose tolerance induced by the HFHC diet at 12 weeks (Figure IIA and IIC in the online-only Data Supplement). GW1516 intervention reversed both fasting hyperinsulinemia and impaired insulin tolerance induced by the HFHC diet, demonstrating normalization of whole-body insulin sensitivity (Figure IIB and IID in the online-only Data Supplement). This is consistent with the improved glucose tolerance in high-fat diet-fed C57BL/6J mice and improved insulin tolerance in *db/db* mice after a 2-week intervention with GW1516.²¹

GW1516 Attenuates Aortic Sinus Atherosclerosis and Aortic Inflammation in HFHC-Fed *Ldlr*^{-/-} mice

Examination of aortic sinus atherosclerosis revealed that oil red-O-stained lesion area of HFHC-fed mice at 4 weeks progressed significantly (≈6-fold) by week 12 (Figure 2A and 2C). In contrast, although lesion area continued to increase, the area was significantly attenuated in GW1516 intervention mice by ≈33% compared with animals remaining on HFHC alone (Figure 2C). GW1516 intervention influenced lesion composition. As a percent of total area, lesions of HFHC-fed animals at either 4 or 12 weeks displayed accumulation of monocyte and macrophage antibody-2-positive macrophages, which was significantly attenuated by intervention with GW1516 (representative images are shown in Figure III in the online-only Data Supplement, and

quantification is shown in Figure 2D). No appreciable smooth muscle (SM) α -actin or collagen deposition was observed in lesions of HFHC-fed mice at 4 weeks, and values were low in 12-week chow-fed mice (Figure 2E; Figure III in the online-only Data Supplement). However, SM α -actin occupied 40% of lesion area in HFHC-fed mice at 12 weeks, which was similar to that of GW1516 intervention mice. As assessed by trichrome staining, the HFHC diet at 12 weeks increased collagen deposition to 25% of lesion area, which was further increased (to 35%) in GW1516 intervention mice (data not shown), despite no further effect on percent lesion SM cell content (Figure 2E; Figure III in the online-only Data Supplement).

To further elucidate the effect of GW1516 intervention on lesion collagen, picrosirius red-stained aortic sinus sections were imaged with circular polarization microscopy to detect fibrillar collagen²² (Figure 2B). The collagen area fraction of lesions was 24% in HFHC-fed animals and 31% in lesions of mice subjected to GW1516 intervention (P=0.025; Figure 2F). This technique also revealed that a collagen-containing fibrous cap existed in lesions in both circumstances (Figure 2B). To determine whether collagen fiber integrity in the cap was affected by GW1516 intervention, collagen birefringence was quantified (Figure 2B and 2G). This revealed a significant 36% increase in the retardation of polarized light by lesion cap collagen in mice subjected to GW1516 intervention (Figure 2G), denoting more densely packed and aligned collagen fibrils (Figure 2B, arrows). Lesion apoptosis, assessed by cleaved caspase-3 staining, was detected in 1.7% of cells within lesions from 12-week HFHC-fed mice (Figure 2H; Figure IV in the online-only Data Supplement). GW1516 intervention significantly reduced cleaved caspase-3 staining to 1.0% of cells (P<0.05), indicating a reduction in

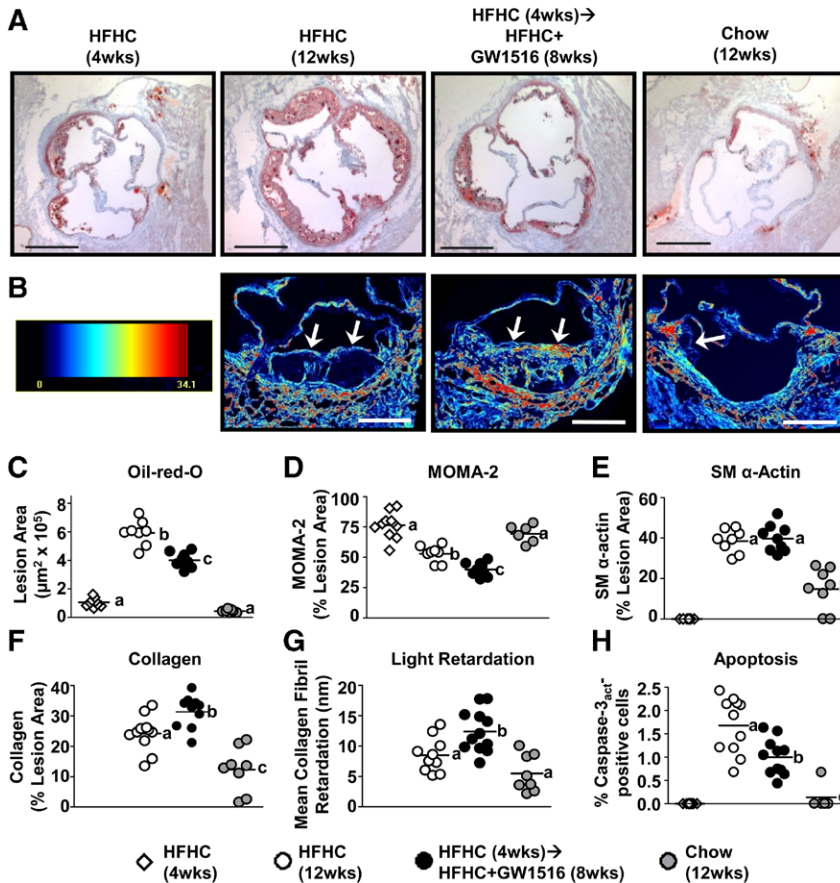


Figure 2. GW1516 attenuates high-fat, high-cholesterol (HFHC)-induced atherosclerosis. **A**, Representative photomicrographs of aortic sinus sections stained with oil red-O and counterstained with hematoxylin. Scale bar, 500 μ m. **B**, Representative photomicrographs of aortic sinus sections stained with picosirius red and imaged using circularly polarizing light and liquid crystal compensation. Scale bar, 250 μ m. Arrows depict birefringent collagen fibers on the surface of atherosclerotic lesions, consistent with fibrous caps of varying organization. Color encoding of light retardation (nm) is depicted in the gradient map (blue: low; red: high). **C**, Quantification of neutral lipid area (oil red-O); **(D)** MOMA-2 (macrophages) and **(E)** smooth muscle (SM) α -actin (smooth muscle cells) expressed as lesion area (oil red-O) or % lesion area (MOMA-2, SM α -actin; n=6–9/group). Representative photomicrographs are available in Figure III in the online-only Data Supplement for MOMA-2 and SM α -actin. **F** and **G**, Quantification of collagen expressed as % lesion area (**F**) and mean collagen fibril light retardation (**G**), determined from picosirius red-stained sections (**B**) and visualization using circularly polarized light (n=8–12/group). **H**, Quantification of lesion apoptosis determined by % caspase-3_{act}-positive cells relative to total cells in aortic sinus lesions (n=5–11/group). Representative photomicrographs are available in Figure IV in the online-only Data Supplement. Staining for collagen, SM α -actin, and caspase-3_{act}-positive cells was undetectable in lesions

from HFHC 4-week sections. Values from individual mice are represented by symbols, and the mean is indicated by a single horizontal line. Different letters indicate significant differences ($P < 0.05$).

apoptotic cells within lesions. Caspase-3_{act}-positive cells were undetectable in sections from 4-week HFHC-fed mice and low in chow-fed mice at 12 weeks.

Lipid analyses of full-length aortae from HFHC-fed mice at 12 weeks revealed that TG and total cholesterol mass increased 1.4-fold and 1.6-fold compared with HFHC-fed mice at 4 weeks (Figure 3A and 3B). GW1516 supplementation decreased aortic TG by 60% compared with the 12-week HFHC cohort and by 40% compared with the 4-week HFHC-fed mice, but the latter was not significant. GW1516 decreased aortic total cholesterol by 27% compared with HFHC-fed mice at 12 weeks, but values remained elevated (30%) compared with HFHC-fed mice at 4 weeks. Collectively, these analyses indicate that GW1516 intervention attenuates lesion progression and results in development of smaller, lipid-depleted, more stable lesions.

A panel of cytokines known to modulate atherogenesis was examined in full-length aortae. After 4 weeks of HFHC feeding, only chemokine (C-C motif) ligand 3 (*Ccl3*) and intercellular adhesion molecule-1 (*Icam1*) expressions were increased compared with chow-fed controls, which is indicative of monocyte recruitment without overt inflammation (Figure 3C). However, the expression of proinflammatory M1 cytokines *Ccl3*, *Il1b*, *Icam1*, tumor necrosis factor (*Tnf*), *Il6*, and chemokine (C-C motif) ligand 2 (*Ccl2*) was markedly induced (2- to 25-fold) in the aortae of HFHC-fed mice at 12 weeks. In contrast, although all cytokines were elevated in GW1516-treated mice compared with HFHC-fed mice at

4 weeks, cytokine expression was significantly lower (–25% to –85%; mean, –60%) compared with HFHC-fed mice at 12 weeks (Figure 3C). Although monocyte and macrophage antibody-2-stained macrophages within lesions decreased \approx 25% in GW1516-treated mice, the greater reduction in cytokine expression suggests that macrophages remaining in lesions of GW1516-treated mice were less inflammatory. Furthermore, compared with 4 weeks, 12-week HFHC feeding significantly increased the aortic expression of the M1 marker inducible nitric oxide synthase (*iNos*) (3-fold) and suppressed the expression of the anti-inflammatory M2 marker arginase 1 (*Arg1*) (–53%), resulting in an exacerbated *iNos/Arg1* ratio (20-fold; Figure 3D). GW1516 intervention completely reversed this expression pattern. Together, these data indicate that in PPAR δ agonist-treated mice, lesion macrophage content is lower (Figure 2D) and there is a shift from M1 to M2 cytokine expression, suggesting an increase in the proportion of macrophages with M2 polarization.

We examined cell signaling cascades known to regulate the macrophage inflammatory response.⁶ Compared with HFHC-fed mice at 4 weeks, activation of extracellular signal-regulated kinase 1/2 and p38 was observed in full-length aortae of HFHC-fed mice at 12 weeks (Figure 4A). Phosphorylated extracellular signal-regulated kinase 1/2 and phosphorylated p38 were significantly lower in GW1516-treated mice, indicating that GW intervention inhibits the development of activated MAPK signaling. We observed a marked induction of aortic

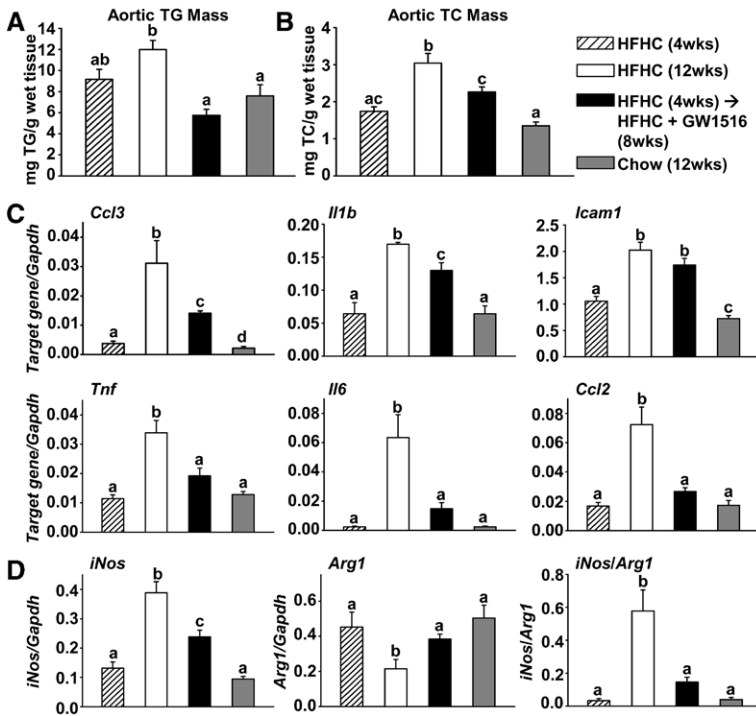


Figure 3. GW1516 attenuates lipid accumulation and M1 macrophage markers and induces a shift toward M2 macrophage markers in full-length aortae. **A** and **B**, Triglyceride (TG) and total cholesterol (TC) concentrations were determined in aortic extracts (n=5–7/group). **C**, mRNA abundance of the indicated proinflammatory M1 cytokines and **(D)** the anti-inflammatory M2 cytokine *Arg1* and the *Arg1/iNos* ratio, determined in full-length aortae dissected free of fat and connective tissue (n=4–6/group). Data are presented as mean±SEM. Different letters indicate significant differences (P<0.05). HFHC indicates the high fat, high cholesterol diet.

NF-κB signaling in HFHC-fed mice at 12 weeks, as demonstrated by increased phosphorylated inhibitor of nuclear factor κ-B kinase and phosphorylated inhibitor of nuclear factor of κ light chain gene enhancer in B-cells, α (Figure 4B). In contrast, GW1516 intervention attenuates NF-κB activation (Figure 4B). This suggests that GW1516 diminishes aortic inflammation, in part, by attenuating diet-induced activation of inflammatory signaling cascades.

GW1516 Intervention Corrects Diet-Induced Aortic Insulin Signaling and ER Stress and Exerts PPARδ-Specific Vessel Wall Effects

Genetic manipulations resulting in impaired insulin signaling in hematopoietic cells exacerbate atherosclerosis, partly

because of increased aortic inflammation and ER stress.^{4,9,10} We, therefore, hypothesized that impaired aortic insulin signaling contributed to the proinflammatory phenotype of aortae in HFHC-fed mice. Aortic phosphorylated Akt and phosphorylated FoxO1 in fasted and acutely refeed mice were examined after the 8-week intervention phase. Compared with chow-fed mice, phosphorylated Akt and phosphorylated FoxO1 were higher in aortae from fasted HFHC-fed mice, but in contrast to chow-fed mice were not further increased by refeeding (Figure 5A). GW1516 intervention completely restored the fasting-to-feeding dynamic regulation of phosphorylated Akt and phosphorylated FoxO1 to patterns observed in chow-fed controls (Figure 5A). The Src homology 2 domain-containing tyrosine phosphatase-1 is primarily expressed

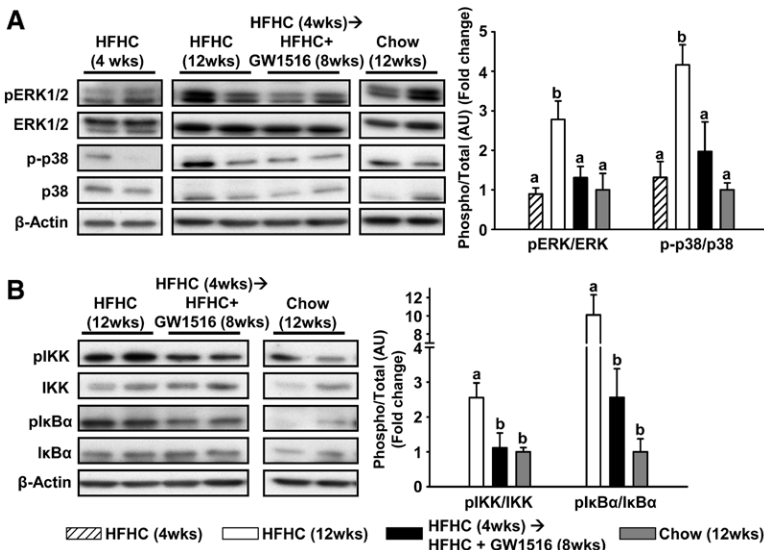


Figure 4. GW1516 corrects aberrant mitogen-activated protein kinase and nuclear factor-κB signaling in full-length aortae of high-fat, high-cholesterol (HFHC)-fed mice. **A**, Representative immunoblots of phosphorylated (p) extracellular signal-regulated kinase (ERK) 1/2 and p-p38 with quantification (mean±SEM) for n=4 to 6/group. Bands from HFHC-fed mice at 4 weeks are from a different immunoblot, whereas bands for the other groups are from the same immunoblot cut from different regions. **B**, Representative immunoblots of pIKK and plkBα with quantification (mean±SEM) for n=4 to 6/group. Representative bands are from the same immunoblot cut from different regions. **A** and **B**, Results are expressed as fold change relative to values for chow-fed mice at 12 weeks. Different letters indicate significant differences (P<0.05).

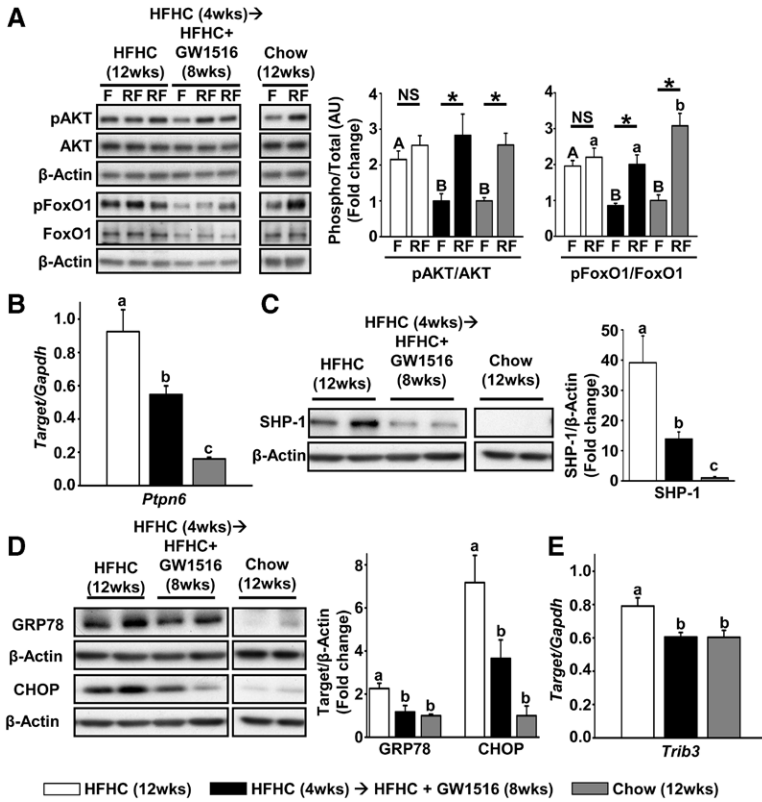


Figure 5. GW1516 corrects aberrant insulin signaling and endoplasmic reticulum (ER) stress in aortae of high-fat, high-cholesterol (HFHC)-fed mice. Immunoblotting or quantitative reverse transcription-polymerase chain reaction was performed on full-length aortae. **A**, Representative immunoblots of phosphorylated AKT (pAKT) and phosphorylated forkhead box O1 (pFoxO1) in aortae from 1 mouse fasted for 16 h (designated F) and 1 or 2 mice fasted for 16 h followed by a 2-h refeeding period (designated RF). Quantification is shown for n=6 to 8/group. **B**, mRNA abundance of the negative regulator of insulin signaling *Ptpn6* (n=4–6/group). **C**, Representative immunoblots of Src homology 2 domain-containing tyrosine phosphatase (SHP-1; the protein product of *Ptpn6*). Quantification is shown for n=4 to 6/group. **D**, Representative immunoblots of ER stress markers GRP78 and CHOP. Quantification is shown for n=4 to 6/group. **E**, mRNA abundance of the negative regulator of insulin signaling *Trib3* (n=4–6/group). Data are presented as mean \pm SEM. **A**, **C**, and **D**, For immunoblot quantification, results are presented as fold change relative to values for chow-fed mice at 12 weeks. In **A**, different upper case letters indicate statistical significance among fasted animals, different lower case letters indicate statistical significance among refed animals, and an asterisk (*) indicates statistical significance between fasted and refed mice within the same diet ($P < 0.05$). In **B** to **E**, different letters indicate significant differences ($P < 0.05$). Representative bands are from the same immunoblot cut from different regions.

by hematopoietic cells and is a known negative regulator of hepatic insulin signaling.²³ Aortae from HFHC-fed mice at 12 weeks were significantly enriched for the Src homology 2 domain-containing tyrosine phosphatase-1 transcript (*Ptpn6*; 5-fold) and Src homology 2 domain-containing tyrosine phosphatase-1 protein (30-fold), both of which were strongly attenuated by GW1516 intervention (Figure 5B and 5C).

Concomitant with dysregulated aortic insulin signaling was a significant increase in ER stress markers GRP78 and CHOP in aortae of HFHC-fed mice at 12 weeks (Figure 5D). The CHOP target gene and negative regulator of insulin signaling, tribbles homolog 3 (*Trib3*),²⁴ was also elevated (Figure 5E). GW1516 intervention restored GRP78, CHOP, and *Trib3* to levels observed in chow-fed controls (Figure 5D and 5E).

To determine whether GW1516 exerted effects directly within the aorta, we examined the expression of known PPAR δ target genes. Expression of adipose differentiation related protein (*Adfp*), angiopoietin-like 4 (*Angptl4*), and carnitine palmitoyltransferase (*Cpt1a*) was significantly increased in aortae of GW1516-treated mice compared with HFHC-fed mice or chow-fed controls at 12 weeks (Figure 6A). Expression of target genes specific for PPAR α (acyl-CoA oxidase [*Acox*]) and PPAR γ (lipoprotein lipase [*Lpl*] and fatty acid binding protein 4 [*Fabp4*]) was unaffected by GW1516 intervention (Figure 6B). Similar results were observed in liver (data not shown). This indicates that GW1516 exerts a direct effect on the arterial wall, which likely contributes to attenuation of aortic inflammation, insulin resistance, and ER stress, as well as

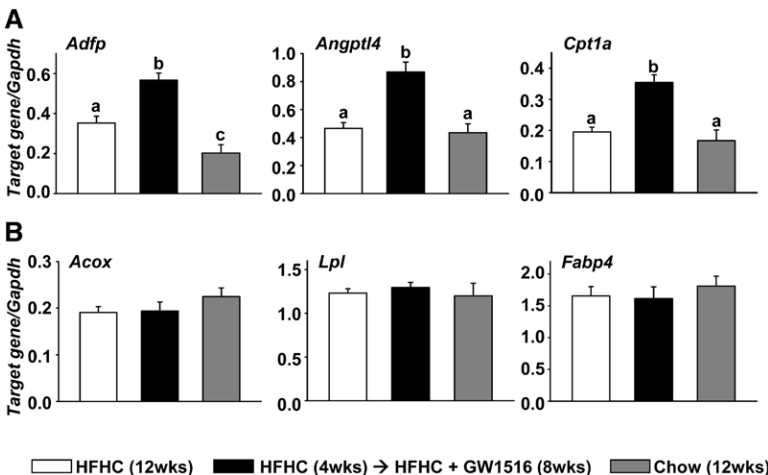


Figure 6. GW1516 activates aortic peroxisome proliferator-activated receptor (PPAR) δ but not PPAR α or PPAR γ . **A**, mRNA abundance of PPAR δ target genes *Adfp*, *Angptl4*, and *Cpt1a* and **(B)** PPAR α target genes *Acox* and *Lpl* and the PPAR γ target gene *Fabp4* in full-length aortae (n=4–6/group). Data are presented as mean \pm SEM. Different letters indicate significant differences ($P < 0.05$). HFHC indicates the high fat, high cholesterol diet.

lesion progression. These data further indicate that with respect to PPARs, the aortic effects of GW1516 are PPAR δ specific.

Discussion

The risk of atherosclerosis is elevated approximately 4-fold in adults with type 2 diabetes mellitus.¹ Despite this, therapeutic strategies to alleviate atherosclerosis associated with insulin-resistant syndromes remain sparse. Here, we demonstrate in mice that intervention with a synthetic PPAR δ agonist, in the context of diet-induced dyslipidemia and insulin resistance, attenuates the progression of early stage lesions to larger plaques. PPAR δ activation was associated with beneficial changes in lesion composition, including fewer macrophages, increased expression of M2 markers, less lipid, increased collagen, decreased ER stress, and fewer apoptotic cells, characteristic of lesions with a more stable phenotype. Furthermore, we show that in HFHC-fed mice, the aberrant inflammatory response and impaired insulin signaling within the aorta are reversed by PPAR δ activation.

Dyslipidemia associated with insulin resistance is characterized by elevated plasma VLDL and LDL, concomitant with reduced plasma high-density lipoprotein.³ Although statins effectively lower plasma LDL, they do not fully correct other features of atherosclerosis risk, namely elevated plasma VLDL, decreased high-density lipoprotein, insulin resistance, and body fat composition.²⁵ The present study demonstrates that intervention by a PPAR δ agonist corrects previously established metabolic disturbances. Although plasma LDL cholesterol was modestly reduced, PPAR δ activation primarily targeted plasma VLDL and high-density lipoprotein. This is consistent with human studies demonstrating that PPAR δ agonists correct mixed dyslipidemia in patients with metabolic syndrome.^{26,27} The current study contributes to the plausibility of PPAR δ agonists as therapeutic agents for metabolic dysregulation associated with insulin resistance. Whether PPAR δ agonists will have an effect in a setting where elevated LDL is a primary determinant of atherosclerosis remains to be determined.

We recently demonstrated in cultured macrophages that PPAR δ activation attenuates VLDL-induced TG accumulation and proinflammatory cytokine expression.¹⁴ We extend these in vitro findings, demonstrating that GW1516 intervention prevents further increase in aortic TG, in concert with significant induction of the PPAR δ target genes *Angptl4* and *Cpt1a*. This suggests that GW1516 may stimulate aortic fatty acid β -oxidation and inhibit aortic lipoprotein lipase activity, thus contributing to reduced atherogenesis. We provide evidence that inflammatory cells within the aortae of HFHC-fed animals were polarized to the proinflammatory M1 phenotype.^{28,29} Furthermore, GW1516 intervention increased the anti-inflammatory M2 state,^{28,29} consistent with reports demonstrating that alternative M2 activation of adipose tissue macrophages and hepatic Kupffer cells is, in part, mediated by PPAR δ .^{30,31} M2 macrophages are thought to contribute to tissue remodeling and repair²⁹ and are increased in lesions undergoing regression.³² Although GW1516 did not induce size regression of early lesions, the M2 phenotype was associated with significant slowing of lesion progression. Longer-term studies are required to assess the effect of PPAR δ

agonists on more advanced stage lesions. Nevertheless, the present study demonstrates that PPAR δ activation alleviates aortic lipid accumulation and inflammation, thus contributing to attenuated lesion development.

That GW1516 increased lesion collagen deposition without altering percent SM cell content is possibly as a result of PPAR δ activation of the synthesis and deposition of extracellular matrix by lesion SM cells. This hypothesis is consistent with a report that PPAR δ activation in cultured vascular SM cells inhibits IL-1 β -induced matrix metalloproteinase-2 and matrix metalloproteinase-9 expression.³³ Reduced lipid deposition in vascular SM cells restores their capacity to elaborate extracellular matrix.^{34,35} Thus, the ability of PPAR δ agonists to improve the function of lipid-loaded vascular SM cells merits further attention.

The MAPK and NF- κ B signaling pathways regulate inflammatory cytokine expression.⁶ In the aortae of HFHC-fed animals, both signaling cascades were significantly activated. GW1516 intervention substantially blunted these changes. In cultured cardiomyocytes, the PPAR δ agonist GW0742 attenuated lipopolysaccharide-induced NF- κ B activation through increased I κ B expression, thereby inhibiting nuclear translocation of NF- κ B.³⁶ We did not observe appreciable changes in total aortic I κ B protein. Thus, the mechanism by which PPAR δ inhibits NF- κ B activation in the context of aortic inflammation remains to be determined. With respect to MAPK activation, GW0742 inhibited angiotensin II-induced phosphorylation of extracellular signal-regulated kinase 1/2 and p38 in cultured mouse macrophages via upregulation of regulator of G-protein signaling (*Rgs*)-4 and *Rgs*5.¹⁹ Consistent with this report, we observed a significant upregulation of both *Rgs*4 and *Rgs*5 in aortae of GW1516-treated mice compared with aortae of HFHC-fed mice (Figure V in the online-only Data Supplement). Collectively, our intervention studies suggest that PPAR δ activation within the aorta dampens inflammatory signaling, leading to attenuation of inflammatory cytokine expression.

Impaired insulin signaling in the vasculature has emerged as a major contributor to lesion progression.⁴ In mice, macrophage deletion of the insulin receptor accelerated the development of advanced lesions,¹⁰ and loss of Akt1 led to severe atherosclerosis.⁹ Endothelial cell-specific deletion of 3 FoxO isoforms resulted in atheroprotection, attributed, in part, to an anti-inflammatory effect.³⁷ Although these gene deletion models highlight the significance of vascular insulin signaling in atherogenesis, these studies do not identify whether insulin signaling becomes dysregulated during lesion development.³⁸ Here, we demonstrate that mice with diet-induced atherosclerosis exhibit impaired aortic insulin signaling, as evidenced by loss of dynamic fasting-to-refeeding regulation of both Akt and FoxO1 phosphorylation, coupled to an induction of negative regulators of insulin signaling, Src homology 2 domain-containing tyrosine phosphatase-1²³ and *Trib3*.²⁴ This suggests that the loss of insulin regulation of both Akt and FoxO1 results in FoxO1 target genes such as *Il1b*⁷ being chronically transcribed rather than dynamically regulated. This mechanism may contribute to the accumulation of proinflammatory mediators within the vessel wall, inducing a state of chronic low-grade inflammation. Impaired aortic insulin

signaling was also correlated with elevations in ER stress markers GRP78 and CHOP. Furthermore, activation of aortic PPAR δ restored dynamic insulin signaling and attenuated ER stress. It is important to note that the presence of arterial insulin resistance did not impair the ability of GW1516 to attenuate pre-established lesion progression. Thus, although difficult to quantify, it remains possible that improved insulin signaling within GW1516-treated aortae contributes to atheroprotection.

In this study, a major factor in the attenuation of lesion development by intervention with GW1516 is reduction of plasma lipids, particularly VLDL/intermediate-density lipoprotein, thereby reducing the atherogenic stimulus. However, we demonstrate that in the aorta, GW1516 stimulates PPAR δ -specific target genes, which are known to improve macrophage lipid homeostasis and attenuate the inflammatory response. Although these effects likely contribute to the observed reduction in atherosclerosis, further studies are required to elucidate the extent to which improved metabolic parameters versus direct vessel wall effects contribute to PPAR δ -mediated atheroprotection. Nevertheless, the current study provides strong evidence that intervention to an HFHC diet with a PPAR δ agonist suppresses and favorably modifies the HFHC diet-induced progression of early lesions. It will be important to determine whether intervention by PPAR δ activation improves the pathology of more advanced lesions and whether extended treatment achieves regression. We conclude that PPAR δ activation remains a viable therapeutic target for atherosclerosis prevention and treatment.

Sources of Funding

This work was supported by grants to M.W. Huff from the Canadian Institutes of Health Research (MOP-126045), the Heart and Stroke Foundation of Canada (PRG-5967), and the University of Western Ontario Department of Medicine (POEM). J.G. Pickering holds the Heart and Stroke Foundation of Ontario/Barnett-Ivey Chair at the Robarts Research Institute. L.A. Bojic held an Ontario Graduate Scholarship.

Disclosures

None.

References

1. Fox CS, Coady S, Sorlie PD, D'Agostino RB Sr, Pencina MJ, Vasan RS, Meigs JB, Levy D, Savage PJ. Increasing cardiovascular disease burden due to diabetes mellitus: the Framingham Heart Study. *Circulation*. 2007;115:1544–1550.
2. Tabas I, Williams KJ, Borén J. Subendothelial lipoprotein retention as the initiating process in atherosclerosis: update and therapeutic implications. *Circulation*. 2007;116:1832–1844.
3. DeFronzo RA. Insulin resistance, lipotoxicity, type 2 diabetes and atherosclerosis: the missing links. The Claude Bernard Lecture 2009. *Diabetologia*. 2010;53:1270–1287.
4. Tabas I, Tall A, Accili D. The impact of macrophage insulin resistance on advanced atherosclerotic plaque progression. *Circ Res*. 2010;106:58–67.
5. Kearney PM, Blackwell L, Collins R, Keech A, Simes J, Peto R, Armitage J, Baigent C. Efficacy of cholesterol-lowering therapy in 18,686 people with diabetes in 14 randomised trials of statins: a meta-analysis. *Lancet*. 2008;371:117–125.
6. Moore KJ, Tabas I. Macrophages in the pathogenesis of atherosclerosis. *Cell*. 2011;145:341–355.
7. Su D, Coudriet GM, Hyun Kim D, Lu Y, Perdomo G, Qu S, Slusher S, Tse HM, Piganelli J, Giannoukakis N, Zhang J, Dong HH. FoxO1 links insulin resistance to proinflammatory cytokine IL-1 β production in macrophages. *Diabetes*. 2009;58:2624–2633.
8. Baumgartl J, Baudler S, Scherner M, Babaev V, Makowski L, Suttles J, McDuffie M, Tobe K, Kadowaki T, Fazio S, Kahn CR, Hotamisligil GS, Krone W, Linton M, Brüning JC. Myeloid lineage cell-restricted insulin resistance protects apolipoproteinE-deficient mice against atherosclerosis. *Cell Metab*. 2006;3:247–256.
9. Fernández-Hernando C, Ackah E, Yu J, Suárez Y, Murata T, Iwakiri Y, Prendergast J, Miao RQ, Birnbaum MJ, Sessa WC. Loss of Akt1 leads to severe atherosclerosis and occlusive coronary artery disease. *Cell Metab*. 2007;6:446–457.
10. Han S, Liang CP, DeVries-Seimon T, Ranalletta M, Welch CL, Collins-Fletcher K, Accili D, Tabas I, Tall AR. Macrophage insulin receptor deficiency increases ER stress-induced apoptosis and necrotic core formation in advanced atherosclerotic lesions. *Cell Metab*. 2006;3:257–266.
11. Burke AP, Kolodgie FD, Zieske A, Fowler DR, Weber DK, Varghese PJ, Farb A, Virmani R. Morphologic findings of coronary atherosclerotic plaques in diabetics: a postmortem study. *Arterioscler Thromb Vasc Biol*. 2004;24:1266–1271.
12. Wahli W, Michalik L. PPARs at the crossroads of lipid signaling and inflammation. *Trends Endocrinol Metab*. 2012;23:351–363.
13. Barish GD, Narkar VA, Evans RM. PPAR delta: a dagger in the heart of the metabolic syndrome. *J Clin Invest*. 2006;116:590–597.
14. Bojic LA, Sawyez CG, Telford DE, Edwards JY, Hegele RA, Huff MW. Activation of peroxisome proliferator-activated receptor δ inhibits human macrophage foam cell formation and the inflammatory response induced by very low-density lipoprotein. *Arterioscler Thromb Vasc Biol*. 2012;32:2919–2928.
15. Lee CH, Chawla A, Urbiztondo N, Liao D, Boisvert WA, Evans RM, Curtiss LK. Transcriptional repression of atherogenic inflammation: modulation by PPARdelta. *Science*. 2003;302:453–457.
16. Li AC, Binder CJ, Gutierrez A, Brown KK, Plotkin CR, Pattison JW, Valledor AF, Davis RA, Willson TM, Witztum JL, Palinski W, Glass CK. Differential inhibition of macrophage foam-cell formation and atherosclerosis in mice by PPARalpha, beta/delta, and gamma. *J Clin Invest*. 2004;114:1564–1576.
17. Graham TL, Mookherjee C, Suckling KE, Palmer CN, Patel L. The PPARdelta agonist GW0742X reduces atherosclerosis in LDLR(-/-) mice. *Atherosclerosis*. 2005;181:29–37.
18. Barish GD, Atkins AR, Downes M, Olson P, Chong LW, Nelson M, Zou Y, Hwang H, Kang H, Curtiss L, Evans RM, Lee CH. PPARdelta regulates multiple proinflammatory pathways to suppress atherosclerosis. *Proc Natl Acad Sci U S A*. 2008;105:4271–4276.
19. Takata Y, Liu J, Yin F, Collins AR, Lyon CJ, Lee CH, Atkins AR, Downes M, Barish GD, Evans RM, Hsueh WA, Tangirala RK. PPARdelta-mediated antiinflammatory mechanisms inhibit angiotensin II-accelerated atherosclerosis. *Proc Natl Acad Sci U S A*. 2008;105:4277–4282.
20. Sznajdman ML, Haffner CD, Maloney PR, Fivush A, Chao E, Goreham D, Sierra ML, LeGrumelec C, Xu HE, Montana VG, Lambert MH, Willson TM, Oliver WR Jr, Sternbach DD. Novel selective small molecule agonists for peroxisome proliferator-activated receptor delta (PPARdelta)—synthesis and biological activity. *Bioorg Med Chem Lett*. 2003;13:1517–1521.
21. Lee CH, Olson P, Hevener A, Mehl I, Chong LW, Olefsky JM, Gonzalez FJ, Ham J, Kang H, Peters JM, Evans RM. PPARdelta regulates glucose metabolism and insulin sensitivity. *Proc Natl Acad Sci U S A*. 2006;103:3444–3449.
22. Nong Z, O'Neil C, Lei M, Gros R, Watson A, Rizkalla A, Mequanint K, Li S, Frontini MJ, Feng Q, Pickering JG. Type I collagen cleavage is essential for effective fibrotic repair after myocardial infarction. *Am J Pathol*. 2011;179:2189–2198.
23. Dubois MJ, Bergeron S, Kim HJ, Dombrowski L, Perreault M, Fournès B, Faure R, Olivier M, Beauchemin N, Shulman GI, Siminovitch KA, Kim JK, Marette A. The SHP-1 protein tyrosine phosphatase negatively modulates glucose homeostasis. *Nat Med*. 2006;12:549–556.
24. Du K, Herzig S, Kulkarni RN, Montminy M. TRB3: a tribbles homolog that inhibits Akt/PKB activation by insulin in liver. *Science*. 2003;300:1574–1577.
25. Sattar N, Preiss D, Murray HM, et al. Statins and risk of incident diabetes: a collaborative meta-analysis of randomised statin trials. *Lancet*. 2010;375:735–742.
26. Bays HE, Schwartz S, Littlejohn T 3rd, Kerzner B, Krauss RM, Karpf DB, Choi YJ, Wang X, Naim S, Roberts BK. MBX-8025, a novel peroxisome proliferator receptor-delta agonist: lipid and other metabolic effects in dyslipidemic overweight patients treated with and without atorvastatin. *J Clin Endocrinol Metab*. 2011;96:2889–2897.
27. Ooi EM, Watts GF, Sprecher DL, Chan DC, Barrett PH. Mechanism of action of a peroxisome proliferator-activated receptor (PPAR)-delta agonist on lipoprotein metabolism in dyslipidemic subjects with central obesity. *J Clin Endocrinol Metab*. 2011;96:E1568–E1576.
28. Adamson S, Leitinger N. Phenotypic modulation of macrophages in response to plaque lipids. *Curr Opin Lipidol*. 2011;22:335–342.

29. Gordon S. Alternative activation of macrophages. *Nat Rev Immunol*. 2003;3:23–35.
30. Kang K, Reilly SM, Karabacak V, Gangl MR, Fitzgerald K, Hatano B, Lee CH. Adipocyte-derived Th2 cytokines and myeloid PPARdelta regulate macrophage polarization and insulin sensitivity. *Cell Metab*. 2008;7:485–495.
31. Odegaard JI, Ricardo-Gonzalez RR, Red Eagle A, Vats D, Morel CR, Goforth MH, Subramanian V, Mukundan L, Ferrante AW, Chawla A. Alternative M2 activation of Kupffer cells by PPARdelta ameliorates obesity-induced insulin resistance. *Cell Metab*. 2008;7:496–507.
32. Feig JE, Parathath S, Rong JX, Mick SL, Vengrenyuk Y, Grauer L, Young SG, Fisher EA. Reversal of hyperlipidemia with a genetic switch favorably affects the content and inflammatory state of macrophages in atherosclerotic plaques. *Circulation*. 2011;123:989–998.
33. Kim HJ, Kim MY, Hwang JS, Kim HJ, Lee JH, Chang KC, Kim JH, Han CW, Kim JH, Seo HG. PPARdelta inhibits IL-1beta-stimulated proliferation and migration of vascular smooth muscle cells via up-regulation of IL-1Ra. *Cell Mol Life Sci*. 2010;67:2119–2130.
34. Beyea MM, Reaume S, Sawyez CG, Edwards JY, O'Neil C, Hegele RA, Pickering JG, Huff MW. The oxysterol, 24(S), 25-epoxycholesterol attenuates human smooth muscle-derived foam cell formation via reduced LDL uptake and enhanced cholesterol efflux. *J Am Heart Assoc*. 2012;1:4e000810.
35. Frontini MJ, O'Neil C, Sawyez C, Chan BM, Huff MW, Pickering JG. Lipid incorporation inhibits Src-dependent assembly of fibronectin and type I collagen by vascular smooth muscle cells. *Circ Res*. 2009;104:832–841.
36. Ding G, Cheng L, Qin Q, Frontin S, Yang Q. PPARdelta modulates lipopolysaccharide-induced TNFalpha inflammation signaling in cultured cardiomyocytes. *J Mol Cell Cardiol*. 2006;40:821–828.
37. Tsuchiya K, Tanaka J, Shuiqing Y, Welch CL, DePinho RA, Tabas I, Tall AR, Goldberg IJ, Accili D. FoxOs integrate pleiotropic actions of insulin in vascular endothelium to protect mice from atherosclerosis. *Cell Metab*. 2012;15:372–381.
38. Bomfeldt KE, Tabas I. Insulin resistance, hyperglycemia, and atherosclerosis. *Cell Metab*. 2011;14:575–585.

Significance

Vascular insulin resistance has been postulated to accelerate atherogenesis by increasing inflammation and endoplasmic reticulum stress. The peroxisome proliferator-activated receptor (PPAR) δ is a ligand-dependent transcription factor that regulates insulin sensitivity, lipid homeostasis, and inflammation. We demonstrate for the first time that intervention with a PPAR δ agonist, in the context of diet-induced dyslipidemia and insulin resistance, attenuates the progression of early stage lesions to larger plaques. PPAR δ activation was associated with beneficial changes in lesion composition, including fewer macrophages, increased M2 cytokine expression, less lipid, increased collagen, decreased endoplasmic reticulum stress, and fewer apoptotic cells, characteristic of more stable lesions. Furthermore, we show that in high-fat, high-cholesterol-fed mice, the inflammatory response and insulin signaling within the aorta are impaired, but these abnormalities are reversed by PPAR δ activation. Collectively, these findings highlight a role for PPAR δ agonists in the prevention and treatment of atherosclerosis, even in a setting of pre-established insulin resistance and atherosclerosis.